JOURNAL OF GEOPHYSICAL RESEARCH, VOL. 103, NO. C9, PAGES 18,425–18,436, AUGUST 15, 1998

Numerical studies of the 4-day oscillation in Lake Champlain

Kenneth Hunkins,[1] Thomas O. Manley,[2] Patricia Manley,[3] and James Saylor[4]

Abstract. The summer thermocline of Lake Champlain, which is found at depths of 20–30 m, oscillates with typical vertical amplitudes of 20–40 m and periods of ~4 days. Fluctuations at the ends of the lake are opposite in phase and accompanied in the central lake by strong shears across the thermocline. These are basin-wide baroclinic disturbances which are forced by wind. A numerical, one-dimensional, two-layer, shallow-water model incorporating nonlinear and frictional effects in a rectangular basin forced by wind was first tested with idealized wind impulses. The results do not resemble the observed thermocline motion. However, when this simple model is forced with wind data from a nearby shore site, there is reasonable agreement between the model results and observed long-period thermocline motions in Lake Champlain. Dispersion effects appear to be negligible here. This contrasts with other long, narrow lakes where dispersion effects are important and internal surges are followed by wave trains resembling the soliton solutions of the Korteweg–deVries equation. A possible explanation for the different regime in Lake Champlain may be found in its unique bathymetry with sloping bottom at the ends and numerous embayments on the sides that provide traps to collect wind-driven warm water and then release it slowly during recovery of equilibrium, preventing the formation of steep fronts and soliton wave trains.

1. Introduction

Lakes with elongated and narrow basins are frequently found in previously glaciated regions. Examples are Lake Champlain and the Finger Lakes in the United States, Babine Lake in Canada, and the subalpine lakes of Italy and Switzerland. Long narrow lakes may also have tectonic origins, an example being Loch Ness in Scotland. The narrow width of these lakes constrains currents to flow primarily along the lake axis, simplifying both observational and theoretical investigation. The study of oscillatory currents in long, narrow lakes began with Forel's pioneering researches on Lake Geneva over a century ago and has been the subject of many investigations since that time [*Hutchinson*, 1957].

New interest in long, narrow lakes has been created by recent extensive field studies in Lake Champlain (Figure 1a). Temperature and current measurements extending over 4 years have been obtained with instruments mounted on moorings supported by subsurface floats at a number of sites (Figure 1b). The results of this study show features sufficiently different from those found in studies of other long, narrow lakes to warrant reexamination of the hydrodynamics of such lakes. The principal basin of Lake Champlain is the Main Lake, which extends 117 km northward from Crown Point at its southern end, where it receives inflow from the river-like South Lake to Rouses Point on the Canadian border, where its outlet flows to the St. Lawrence River. The Main Lake has an average breadth of 6.3 km, an average depth of 29 m, and a maximum depth of 122 m. Although the shoreline of the Main Lake is complex and marked by headlands and shallow bays, there is a deep channel with a breadth of about 2 km and relatively smooth sides extending the length of the lake (Figure 1b). This deep trough suggests that a one-dimensional model of the type used here will be useful in describing the basic hydrodynamics of this lake.

The waters of Lake Champlain, like those of most lakes in temperate climates, are stratified during summer and autumn, with a nearly uniform warm layer, the epilimnion, overlying a cold deep layer, the hypolimnion. These two layers are separated by a transition layer, the metalimnion. The thermocline is the surface of the steepest temperature gradient within the metalimnion. Three continuous profiles of temperature and density obtained with a conductivity-temperature-depth profiler (CTD) in midchannel at Thompsons Point are shown in Figure 2. Density, the dynamically important quantity, is derived from temperature using the international equation of state. The typical summer density structure is evident with a shallow epilimnion underlain by a steep gradient of temperature and density which decreases with increasing depth. The epilimnion averages from 10 to 25 m in thickness, increasing in depth as the season progresses from summer to autumn.

The surface of the Main Lake frequently oscillates with a period of 4 hours on a basin-wide scale. These surface oscillations were first identified and discussed by *Myer and Gruendling* [1979]. These investigators also found that the thermocline oscillated with a much longer period of ~4 days. In the more recent field studies, recordings of temperature were made at many levels with thermistor strings on moorings deployed over time spans extending up to 4 years located at the six mooring sites shown in Figure 1b. Results from September 1993 for two moorings at opposite ends of the Main Lake are shown in Figure 3 together with winds at Burlington International Airport. Isotherm levels were calculated from temperatures measured at fixed levels on moorings supplemented by vertical

[1]Lamont-Doherty Earth Observatory of Columbia University, Palisades, New York.
[2]Marine Research Corporation, Middlebury, Vermont.
[3]Department of Geology, Middlebury College, Middlebury, Vermont.
[4]NOAA Great Lakes Environmental Research Laboratory, Ann Arbor, Michigan.

Paper number 98JC01450.
0148-0227/98/98JC-01450$09.00

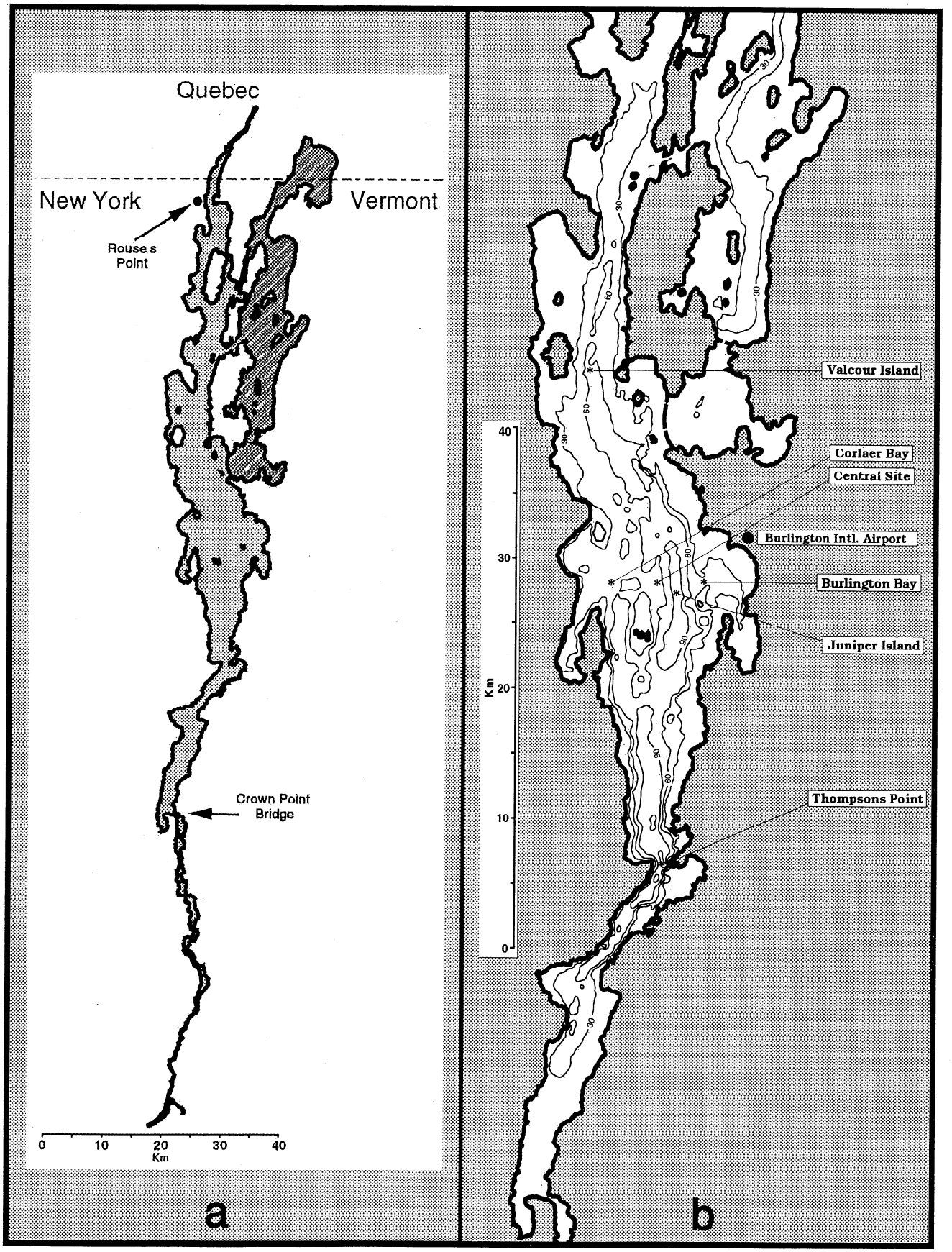

Figure 1. (a) Shoreline of Lake Champlain. The Main Lake (light gray shading) extends from Crown Point Bridge to Rouses Point. Shallow arms of the lake (dark gray shading) are connected to the rest of the lake only by restricted passages and are not part of the Main Lake. (b) Bathymetric chart of Lake Champlain. Depths are in meters. Asterisks indicate sites of instrumented moorings.

gradient information derived from profiles such as those in Figure 2. The thermocline is constantly in motion, moving up and down over a broad range of periods that are much longer than those of surface oscillations. These oscillations of isothermal surfaces show several spectral peaks, with the most prominent peaks centered at periods of 4, 7, and 10 days. Oscillations at these long periods are nearly opposite in phase at the two ends of the lake, with currents in the epilimnion flowing in the opposite direction to those in the hypolimnion. Some correlation between north-south winds and thermocline depth is discernible in the observations shown in Figure 3, but the phase relationships are irregular. The thermocline is often depressed at the northern end (Valcour Island) and elevated at the southern end (Thompsons Point) during periods of strong winds from the south, which typically occur during summer and early autumn. Only the north-south wind component is shown. Little correlation was found between the weaker east-west wind component and thermocline depth. Current meter results, not illustrated here, show strong shears of about 0.5 m/s over a 10-m depth change across the metalimnion. To simplify discussion and comparison with models, the data used in this paper are restricted to these two sites and to the month of September 1993. Expanded discussion of the complete data sets, including further documentation of the observations described here, will be presented in a paper that is in preparation.

Some idea of the importance of these oscillations to water movements in the Main Lake is given by an estimate of the horizontal motions associated with them. A water parcel will be transported up and down the lake basin by the 4-day oscillation and will carry with it any dissolved materials or particulate matter it contains. The excursion distance for the 4-day oscillation can be estimated by assuming that the motion is sinusoidal. Then the velocity along the lake axis will be

$$V = V_0 \sin \omega t$$

where V_0 is the maximum velocity, t is time, and ω is the frequency. The distance D that a water parcel moves either up or down the lake during one half cycle is then

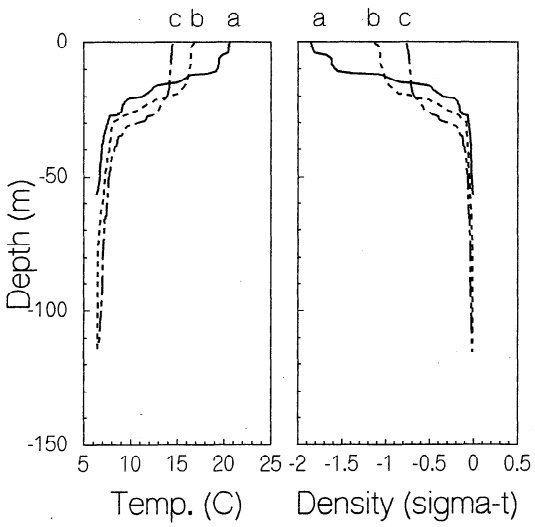

Figure 2. Profiles of temperature and density versus depth on September 4 (solid line), 22 (dashed line), and 29 (dot-dash line) midchannel at Thompsons Point. Here, $\sigma_t = \rho - 10^3$ kg/m^3.

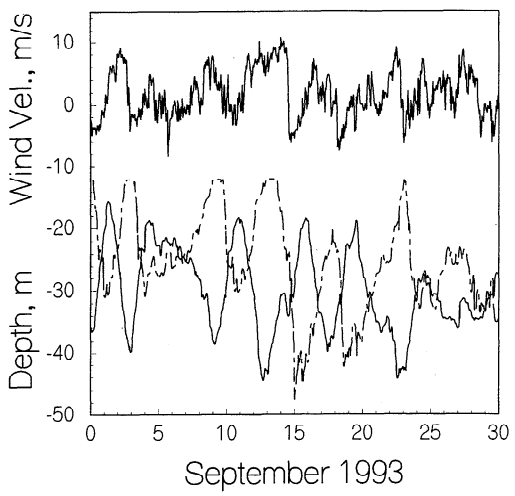

Figure 3. (top) Wind velocity at Burlington airport (north-south component). Positive velocity is directed northward. (bottom) Depth of 10°C isotherm at two sites in Lake Champlain during September 1993. The Valcour Island site (solid line) is near the northern end of the Main Lake, and the Thompsons Point site (dashed line) is near the southern end.

$$D = V_0 \int_0^{\pi} \sin \omega t \, dt = V_0 T/\pi$$

where $T = 2\pi/\omega$ is the period. Typical values of 25 cm/s for the maximum velocity and 100 hours for the period give an excursion distance of 28.7 km. Thus a water parcel is carried northward or southward for a distance almost one-fourth the length of the Main Lake in 2 days' time.

In this paper we take a simple approach and seek to explain these long-period motions of the lake surface and thermocline using only the most basic physics. One- and two-layer numerical models of long narrow basins driven by wind are explored to give insight into response under various conditions. First, response to idealized wind impulses is investigated. Free oscillations result that do not closely resemble the observed response. Then response to actual observed winds is modeled. The forced oscillations which result are found to provide reasonable simulations of the observed thermocline motions.

2. Surface Seiches

Standing waves, in which the surface oscillates on a basin-wide scale, often follow changes in wind speed or direction over lakes. Water is first piled up at the downwind end of the lake by wind drag. Later, after the wind drops or changes direction, lake waters oscillate freely, with periods determined by the basin geometry. Vertical displacements of the surface are in the millimeter to centimeter range, with oscillation periods of minutes to hours. In stratified lakes, internal temperature surfaces may also oscillate as internal seiches. In this case amplitudes and periods are both much greater than those of surface seiches. Vertical displacements of meters to tens of meters and periods of hours to days are observed. Discussions of seiches are found in reviews of physical limnology such as those by *Csanady* [1975], *Imberger and Hamblin* [1982], and *Mortimer* [1979].

The measured periods of surface seiches in lakes are generally found to be in close agreement with periods derived from

linear hydrodynamic theory. One numerical technique, devised by *Defant* [1961], solves the linear shallow-water equations by stepwise integration using the finite-difference method to yield the free period as well as the associated vertical and horizontal motions for one-dimensional lakes of varying cross section. Recently the technique has been applied to the Main Lake to predict a period of 4.0 hours for the fundamental longitudinal mode [*Prigo et al.*, 1995]. This predicted period agrees well with the range of 3.9–4.6 hours observed by *Myer and Gruendling* [1979].

3. Hydrodynamic Equations

The numerical models used here employ simplified versions of the momentum and continuity equations. To facilitate subsequent discussion of the simplifications and their justification, the hydrodynamic equations are reviewed here. The two-dimensional equations for an incompressible fluid of constant density are

$$\frac{\partial v}{\partial t} + v\frac{\partial v}{\partial y} + w\frac{\partial v}{\partial z} = -\frac{1}{\rho}\frac{\partial p}{\partial y} + \frac{1}{\rho}\frac{\partial \tau_{yz}}{\partial z}, \tag{1}$$

$$\frac{\partial w}{\partial t} + v\frac{\partial w}{\partial y} + w\frac{\partial w}{\partial z} = -\frac{1}{\rho}\frac{\partial p}{\partial z} - g, \tag{2}$$

$$\frac{\partial v}{\partial y} + \frac{\partial w}{\partial z} = 0, \tag{3}$$

where v and w are velocities in the y and z directions, respectively. Horizontal shear stress in the y direction due to vertical shear of the horizontal velocity v is represented by τ_{yz}. Other symbols have their usual meanings. The Earth's rotation and stress due to horizontal velocity shear have both been neglected in these equations, although rotation effects will be taken into account later.

4. A One-Layer, One-Dimensional Model

A one-layer model was developed both to model winter behavior and to provide the basis for the two-layer model described later. Consider a long lake with width so narrow that transverse currents may be neglected. The water is homogeneous, corresponding to winter and spring conditions, and the horizontal scale of motion is much greater than the vertical scale. Wind forcing and frictional damping are included, unlike Defant's method, which considers only free oscillations. This one-dimensional model is intended to explore motions in idealized long narrow lakes and cannot simulate the small-scale details of currents within the actual confines of Lake Champlain.

Currents are driven by wind stress at the surface, τ_a, and damped by frictional stress τ_f at the bottom. Since the depth scale is much less than the horizontal scale, vertical velocities are neglected and pressure is hydrostatic. The long axis of the basin is in the y direction, which corresponds to north for Lake Champlain. Equations (1) and (3) are integrated vertically to give the forced shallow-water equations,

$$\frac{\partial v}{\partial t} + v\frac{\partial v}{\partial y} + g\frac{\partial h}{\partial y} = \frac{\tau_a - \tau_f}{\rho_w(H + h)}, \tag{4}$$

$$\frac{\partial h}{\partial t} + \frac{1}{b}\frac{\partial Q}{\partial y} = 0, \tag{5}$$

where $Q = vb(H + h)$ is the volume transport through a cross section and h is the deviation of the surface level from equilibrium. Velocity v is now a vertically averaged value. Cross-sectional area A and breadth at the surface, b, are prescribed for each box. $H = A/b$ is the water depth at rest.

This pair of partial differential equations was solved in finite-difference form using explicit time marching. The lake was divided into a string of boxes that are uniform in length but varying in cross-sectional area and breadth. An advantage of one-dimensional models is their speed of execution on small computers, which allows experiments to be performed rapidly. At each time step, current velocity and surface elevation were calculated sequentially for each box along the length of the lake using (4) and (5). The time step used, 10 s, is less than the time required for a long wave to travel across one box, thus meeting the usual stability criterion. For the nonlinear advective terms, an upwind differencing scheme was employed [*Kowalik and Murty*, 1993]. Neither smoothing nor filtering was performed on the output. The programs described here were written in QuickBASIC language and run on an IBM-PC computer.

Wind and bottom stress were calculated using quadratic drag laws,

$$\tau_a = \rho_a C_{10} W|W| \qquad \tau_f = \rho_w C_f v|v|,$$

where W is axial wind velocity (m/s), $\rho_a = 1.225$ kg/m^3 is air density, $\rho_w = 1000$ kg/m^3 is water density, $C_{10} = 0.0027$ is the surface drag coefficient corresponding to winds measured 10 m above the surface, and $C_f = 0.0025$ is the bottom drag coefficient. The values chosen for the drag coefficients are conventional ones that have been used for successful simulation of lake-wide response to storms on Lake Ontario [*Simons*, 1974, 1975] as well as for prediction of storm surges in shallow seas [*Welander*, 1961].

Shallow-water theory assumes that the wavelength of the motion is much greater than water depth. Since the Main Lake is 117 km long and has a mean depth of only 29 m, this assumption is clearly justified for the lowest modes. Linearization of the equations assumes that vertical displacements are much less than water depth, and this condition is also well justified for surface modes in the Main Lake. This explains the success of linear shallow-water theory in predicting the characteristics of surface motions. However, in the case of internal motions, the second assumption may not be satisfied, and nonlinear effects need further examination. Also the Earth's rotation, which can be shown to have little effect on surface motions, needs further consideration in the case of internal motions.

Two different basin shapes were used with the one-layer model. The first is a rectangular basin measuring 117 km long, 6.3 km wide, and 28.7 m deep that is divided into 100 boxes each 1.17 km long. The second basin shape is a string of boxes of varying dimensions which form a one-dimensional representation of the Main Lake. Values of cross-sectional area and surface breadth for each box are based on recent bathymetric data (B. S. H. Connell, unpublished data, 1994). Dimensions of the rectangular basin are mean values of the 100 boxes. Boundary conditions are no flow through the end sections. Initially, the surface is level and velocity is zero.

Response of surface elevation in the rectangular basin to a wind burst of 10 m/s lasting for 1 hour is shown in Figure 4. During the first hour, water is driven downwind, raising the surface level at the downwind end. When the wind ceases after

1 hour, the lake level has been raised about 2 cm at the downwind end and depressed by a similar amount at the upwind end. Sloping surfaces at the ends of the lake then propagate toward each other. The two waves are mirror images of each other. They reflect back and forth from the ends, crossing and recrossing each other. Corresponding current velocities reach maximum values of about 8 cm/s at the center of the basin. The period of the motion is 3.9 hours, which agrees well with the period given by the formula for linear free-standing waves in a rectangular basin,

$$T = 2L/\sqrt{gH}, \tag{6}$$

where T is the period of longitudinal free oscillations with the lowest mode and L is basin length [*Hutchinson*, 1957].

When Main Lake bathymetry is used, response is more complex as shown in Figure 5. Again, wind blows from south to north for 1 hour. A periodicity of about 4 hours is still evident, particularly at the shallow northern end, but the motion is no longer antisymmetric about the middle of the lake. The greatest response appears at the shallow northern end, where elevation reaches about 10 cm above equilibrium level. Current velocities reach their maximum values of about 15 cm/s within a short distance of the northern end.

These results were obtained with a fully nonlinear model. This model can be linearized by making three changes. In equation (4) the second term is dropped and h is eliminated from the $(H + h)$ term. In (5) we set $Q = vA$. There is no discernible difference between the illustrated results using the nonlinear version and results, not shown here, obtained with a linearized version. This further confirms the adequacy of linear theory for modeling surface motions in long, narrow lakes.

5. Nonlinear Effects

Finite-amplitude waves described by the nonlinear shallow-water equations have a tendency to steepen, since propagation speeds for these waves are proportional to wave height.

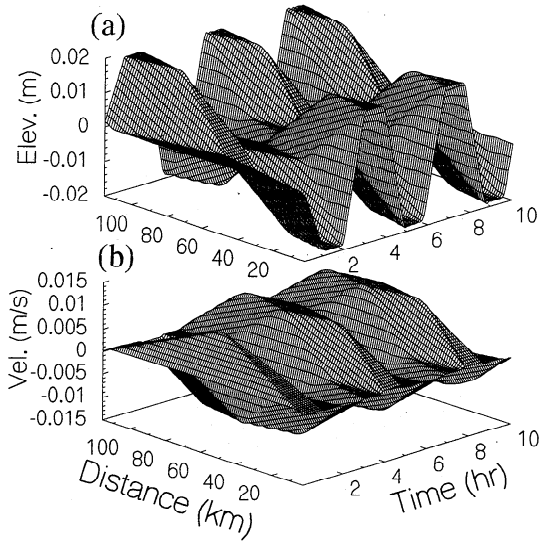

Figure 4. (a) Surface elevation and (b) current velocity in a rectangular basin following a burst of wind for 1 hour at 10 m/s. Wind is directed northward (positive y direction). The rectangular model basin measures 117 km long, 6.3 km wide, and 28.7 m deep. The free period of the lowest mode is 3.9 hours.

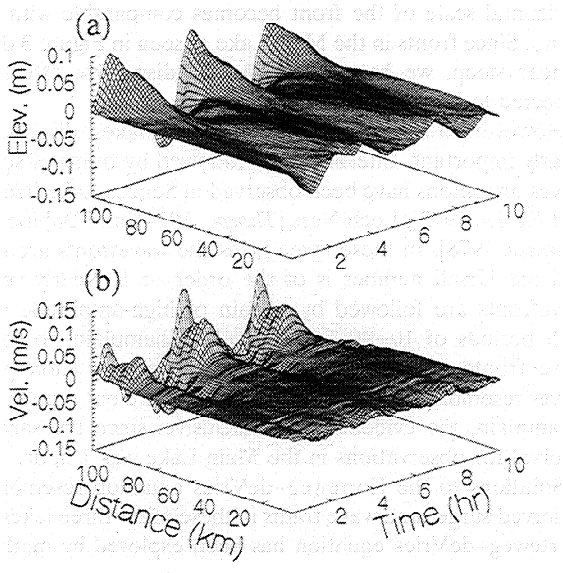

Figure 5. (a) Surface elevation and (b) current velocity in model Main Lake basin following a burst of wind for 1 hour at 10 m/s. Wind is directed northward (positive y direction). Basin bathymetry is modeled on Main Lake of Lake Champlain.

Higher, and therefore faster, waves overtake lower waves ahead of them, leading to steepening at the front of a wave packet. The resulting bores are analogous to shock waves in gases. This steepening tendency is limited by factors that may prevent overturning. In the shallow-water formulation, vertical motions, which are associated with dispersion, have been neglected. When vertical motions are retained in the momentum equations, the tendency of waves to steepen and overturn is counteracted by dispersion. When friction is negligible, the steepening effect is opposed only by dispersion. In this case there may be a balance between nonlinearity and dispersion with waves of permanent form, known as solitary waves and solitons, resulting. A special case of solitary waves is the train of solitons that follows a steepened wavefront [*Whitham*, 1974].

The relative importance of dispersive and nonlinear effects can be assessed with a nondimensional number [*Ursell*, 1953]. The magnitude of dispersion effects is measured by the square of the ratio of layer depth H to a characteristic length λ, which is the length scale over which H and v change appreciably. The magnitude of nonlinear effects is given by the ratio of amplitude a to layer depth H. The relative importance of these two effects in the evolution of finite-amplitude disturbances is measured by the Ursell number U. It is the ratio of nonlinear effects, a/H, to dispersive effects, H^2/λ^2, so that we have

$$U = a(\lambda^2/H^3).$$

For $U \gg 1$ the evolution is governed by nonlinearity, while for $U \ll 1$, dispersion dominates. Solitary waves represent a balance between the two effects when $U \approx 1$.

Although nonlinear effects are negligible for surface seiches, they can be important for internal oscillations. In early summer, when mean depth of the epilimnion is about 15 m, vertical excursions of the thermocline reach 10 m or more in Lake Champlain, and in autumn, when mean depth is about 25 m, excursions of 15 m or more are frequently noted. Thus the nondimensional ratio a/H has a value of about 0.6 for internal motions in this lake. Dispersion effects will be small unless the

horizontal scale of the front becomes comparable with layer depth. Since fronts in the Main Lake as seen in Figure 3 do not appear steep, we have $U \gg 1$ and dispersive effects are expected to be small.

However, in several other long, narrow lakes, dispersion is clearly important. Internal bores followed by trains of solitary waves or solitons have been observed in Seneca Lake [*Hunkins and Fleigel*, 1973], Loch Ness [*Thorpe*, 1974], and Babine Lake [*Farmer*, 1978]. In these three lakes the wavefronts are steep, and the Ursell number is of the order of 1. Nearly vertical wavefronts are followed by a train of high-amplitude waves with periods of 10–40 min. In Lake Champlain no vertical wave fronts are observed. Although trains of short-period waves resembling those in the other lakes are not seen in Lake Champlain, the evidence is inconclusive, since the sampling interval for observations in the Main Lake was 1 hour.

Solutions to the Korteweg–deVries equation resemble the observed surges and wave trains in these other three lakes. The Korteweg–deVries equation has been explored by mathematicians and numerical modelers, and many aspects of its solutions are known [*Whitham*, 1974]. The Korteweg–deVries equations are based on asymptotic expansions of (1)–(3) without friction and balance nonlinear steepening effects with dispersion under conditions of weak nonlinearity. They have been suggested as a basis for modeling thermocline oscillations in these other three lakes. However, for Lake Champlain, where wavefronts are not steep, the shallow-water equations appear to be more appropriate. The reason for the different regime in Lake Champlain is not yet clear. We can only offer a possible explanation. It may be that topographic effects are responsible. At the ends the bottom of Lake Champlain slopes gently upward and there may not be a sufficient reservoir of accumulated water to produce a bore upon release after a wind change. Also, the numerous shallow bays that provide storage for warm upper waters at the downwind end form a distributed source of water after a wind change, again inhibiting bore formation. The other three lakes more closely resemble the rectangular basin of the model, since they have straighter sides and deeper ends than Lake Champlain.

6. Rotational Effects

In the central part of the Main Lake far from shore, current direction has been observed to rotate in a clockwise circle at the Coriolis period. Clearly, the Earth's rotation is important in the dynamics of this lake. Further evidence is found in cross-lake tilts of the thermocline, which are observed to be in the sense expected for geostrophic motion.

Rotational effects become important when the radius of deformation is comparable with or less than the typical horizontal scale of the lake. The radius of deformation,

$$R = \sqrt{gH}/f,$$

is the ratio of the long-wave velocity to the Coriolis parameter f. The Coriolis period, $2\pi/f$, is 17 hours at the latitude of Lake Champlain ($f = 10^{-4}\ s^{-1}$). Using the mean depth for the Main Lake, $H = 29$ m, we find that $R = 168$ km, which is much greater than the mean width of 6.3 km. Thus rotational effects are not of importance for surface (barotropic) motions, and the Coriolis term was not included in the one-layer, one-dimensional model just described. However for two-layer (baroclinic) motions an internal radius of deformation is applicable in which the reduced gravity has a typical value of $g' = 0.01$ m s^{-2}. Depth H now refers to the upper layer which is typically about 25 m. For baroclinic motions the internal radius of deformation is then 5 km, which is comparable with the width of the lake. Rotational effects need to be considered for internal motions.

The numerical models developed here are based on a one-dimensional momentum equation and do not initially include rotation. Rotation leads to transverse currents and hence two-dimensional horizontal motion. If transverse currents were included, a disturbance would produce Kelvin waves traveling cyclonically around the basin. However, since periods of interest here are much longer than the Coriolis period, we may adopt a compromise approach. Currents are assumed to be in geostrophic balance. Rotation effects are introduced into this numerical model by adding a geostrophic correction term to the nonrotating model. Rotation leads to a transverse slope of the surface, which can be approximately represented by the geostrophic relation,

$$fv = g(\partial h/\partial x). \tag{7}$$

Integration yields a correction term for transverse deviation of the surface from its equilibrium height,

$$h_{\text{corr}} = \frac{f}{g} vx. \tag{8}$$

Choose the y axis along the center of the channel. The x axis crosses the channel at midlength. Deviation for the rotating case is

$$h_{\text{rot}} = h + h_{\text{corr}} = h + \frac{f}{g} vx. \tag{9}$$

7. A Rotating, Two-Layer, One-Dimensional Model

The one-layer shallow-water model can be extended to two homogeneous layers separated by an interface. Again, cross-sectional area may vary from section to section. The vertically and laterally integrated equations for each box in this model are

$$\frac{\partial v_1}{\partial t} + v_1 \frac{\partial v_1}{\partial y} + g \frac{\partial h_1}{\partial y} = \frac{\tau_a - \tau_i}{\rho_1(H_1 + h_1 - h_2)}, \tag{10}$$

$$\frac{\partial (h_1 - h_2)}{\partial t} + \frac{1}{b_1} \frac{\partial Q_1}{\partial y} = 0, \tag{11}$$

$$\frac{\partial v_2}{\partial t} + v_2 \frac{\partial v_2}{\partial y} + g \frac{\partial h_1}{\partial y} - g' \frac{\partial (h_1 - h_2)}{\partial y} = \frac{\tau_i - \tau_f}{\rho_2(H_2 + h_2)}, \tag{12}$$

$$\frac{\partial h_2}{\partial t} + \frac{1}{b_2} \frac{\partial Q_2}{\partial y} = 0, \tag{13}$$

where subscripts 1 and 2 refer to the upper and lower layers, respectively. The volume transports in each layer are

$$Q_1 = v_1 b_1 (H_1 + h_1 - h_2),$$

$$Q_2 = v_2 b_2 (H_2 + h_2).$$

This model has vertical end walls against which the model interface abuts. The bottom of Lake Champlain slopes gently upward toward the ends, and the resting thermocline intersects the bottom at some distance from the ends (the thermocline

shore). The two-layered model does not include the shallow, single-layered regions at the ends of the lake. In the numerical experiments to be described, the model is limited in horizontal extent to that part of the lake deeper than 20 m, which is approximately the depth where the thermocline intersects the bottom. This truncates the model to 68 boxes, corresponding to a length of 80 km. The model basin is centered on the Central site and extends northward 40 km to the southern tip of Isle La Motte and southward for 40 km to a section 10 km south of Basin Harbor, Vermont. Initial conditions are zero current, level surface, and level interface. A condition of no flow is prescribed at the end sections, although it may be noted that the actual ends of the Main Lake are partially open.

There is little field or laboratory evidence on which to base a value for interfacial stress. One laboratory study showed interfacial stress to be much smaller than bottom stress [*Turner*, 1973, p. 72]. Calculation of the Richardson number across the thermocline during the large shear flows associated with the 4-day oscillations in Lake Champlain gives values of about 0.33, indicating stable flow. This provides some justification for specifying little or no mixing across the interface. On this limited evidence, interfacial shear stress τ_i is assumed to be negligible for these studies. The two layers are coupled exclusively through the pressure gradients, with frictional dissipation occurring only at the bottom.

8. Response to Idealized Forcing

A wind burst initially transports water in the epilimnion away from the upwind end, where the interface becomes elevated, and moves it toward the downwind end, where the interface becomes depressed. For weak forcing, the response is linear and the waves propagating from the ends are symmetrical. In the example depicted in Figure 6a the wind blows for 1 hour in the negative y direction at a speed of 10 m/s. As the volume of upper layer water increases at the downwind end, the depression of the interface travels in the upwind direction, away from the end. When the wind ceases, recovery toward equilibrium begins. The elevation of the interface at the upwind end and the depression of the interface at the downwind end each continue to propagate away from the respective ends where they originated, crossing each other at the midsection after 27 hours. For this short wind burst the response is linear and wave fronts propagate with similar shapes which do not change. Model parameters for the case shown in Figure 6a are: $H_1 = 25$ m, $H_2 = 50$ m, $g' = 0.01$ ms^{-2}, and $L = 80$ km. The free period of the gravest mode may be calculated from the formula,

$$T = \frac{2L}{\sqrt{g' H_1 H_2/(H_1 + H_2)}}.$$

For this case the free period is 109 hours.

However, in the case of strong forcing when the wind blows for a longer time, deviations of the thermocline from equilibrium grow larger, and the waves propagating from opposite ends are no longer mirror images of each other. Nonlinear effects lead to a distinct asymmetry. This is shown in Figure 6b, where the wind has the same velocity as in the previous example but continues for 12 hours. The wave front steepens as it travels away from the downwind end, developing into an internal surge about halfway down the basin. In analogy with shock waves in compressible gases, this is a wave of compres-

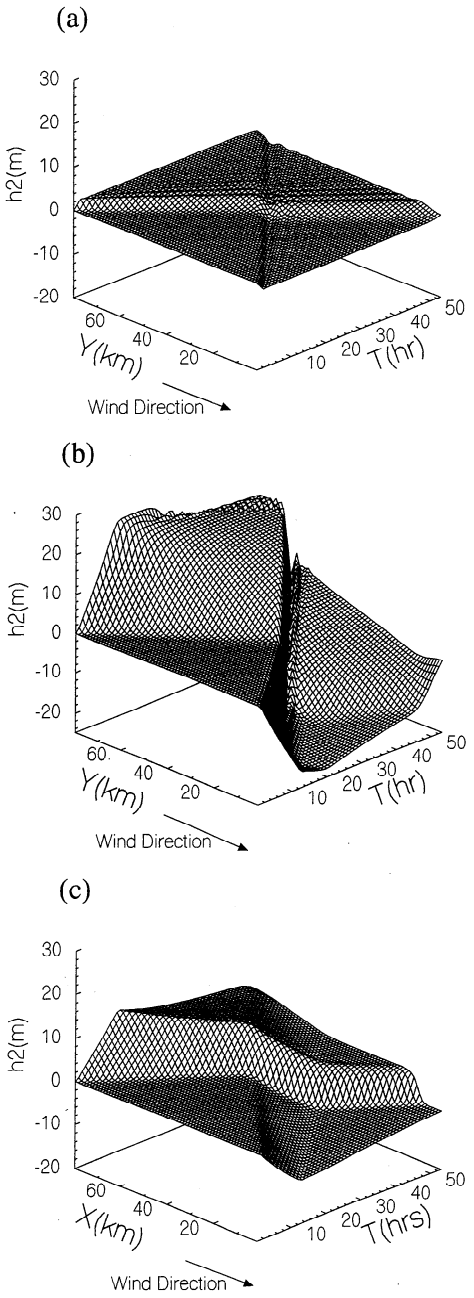

Figure 6. (a) Linear response of the thermocline to weak wind forcing. Interface elevation along the basin axis is shown as a function of time. A wind burst at 10 m/s blows for one hour in the negative y direction shown by the arrow. After the wind drops, a wave of elevation propagates in the same direction as the wind, and a wave of depression propagates in the opposite direction. These waves, propagating in opposite directions, are mirror images of each other. The rectangular model basin measures 80 km long, 5 km wide, and 75 m deep, with $H_1 = 25$ m and $H_2 = 50$ m. Reduced gravity, $g' = 0.01$ m/s^2. The free period is 109 hours for the lowest internal mode. (b) Nonlinear response of the thermocline to strong wind forcing. Model parameters are the same as in Figure 6a except that wind burst lasts for 12 hours. Note that the wavefront propagating in the upwind direction steepens with time while the wavefront propagating downwind becomes less steep with time. (c) Inverted nonlinear response. Model parameters are the same as in Figure 6b except that the upper layer is deeper than the lower layer, $H_1 = 50$ m, and $H_2 = 25$ m. Note that the steepening tendencies of the two waves are opposite those in Figure 6b.

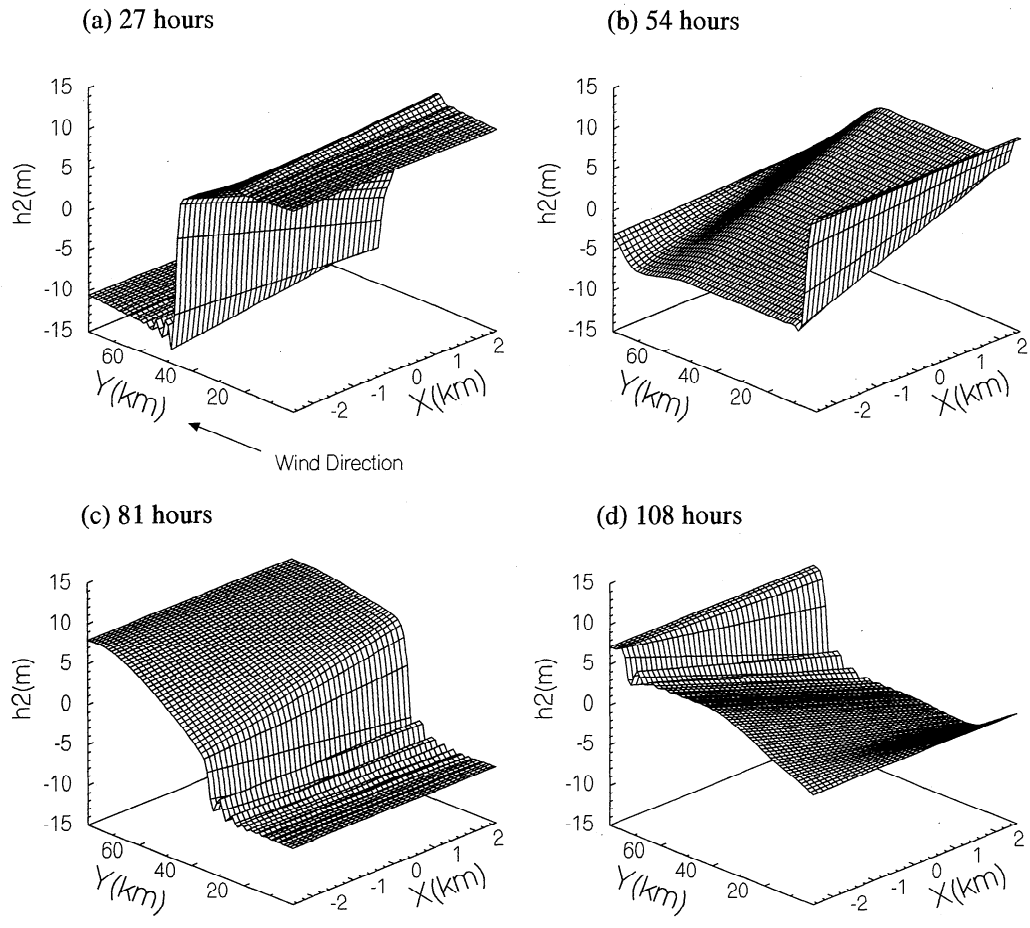

Figure 7. Rotation leading to cross-lake tilting. Interface deviation following a burst of wind is shown at intervals of one-quarter cycle, at (a) 27 hours, (b) 54 hours, (c) 81 hours, and (d) 108 hours. $H_1 = 25$ m and $H_2 = 50$ m. Wind blows for 6 hours at 10 m/s. The free period of the lowest mode is 109 hours.

sion. In contrast, the wave front traveling from the upwind end spreads out as it travels, so that its slope becomes less steep with time. This is analogous to a wave of expansion. These waves reflect back and forth from the ends, completing one round trip in about 109 hours. These are free oscillations or internal seiches, since the wind duration is short in relation to the natural period.

In the two-layer case just illustrated, the resting upper layer was shallower than the resting lower layer. This resembles normal summer conditions in Lake Champlain and in many other deep lakes in temperature climates. However in shallow lakes, or in deep lakes just before overturn in the autumn, the epilimnion may be deeper than the hypolimnion. When the upper layer is deeper than the lower layer, an interesting reversal in direction of the compression and expansion waves occurs. In this case the initial shock wave originates at the upwind end and travels in the same direction as the wind, while the expansion wave originates at the downwind end and travels upwind. This effect is illustrated in Figure 6c.

The change in roles of the two layers can be understood by considering development of an internal surge as a result of amplitude dispersion. Higher, faster waves overtake lower, slower waves. Wave speed is controlled by the depth of the thinner layer. A wind pulse will cause a shallow upper layer to thicken at the downwind end. After the wind stops, a shock wave propagates away from the downwind end, travelling in the upwind direction. However, when the deep layer is initially shallower than the upper layer, the deep layer will thicken upwind as the two layers adjust hydrostatically. After the wind stops, a shock wave propagates away from the upwind end and in the downwind direction. This follows the general principle that shock waves travel only in the direction from high pressure to low pressure.

A third type of response occurs when the two layers are initially equal in depth. In this case, not shown here, there are no surges, only two waves of expansion traveling in opposite directions. This case is related to the lock-exchange problem in which two fluids of equal depth but of different density are initially separated by a barrier. After the barrier is removed, the two fluids flow into opposite basins to seek a new equilibrium as superposed layers [*Hunkins and Whitehead*, 1992].

Only profiles along the central axis of the basin have been shown in the previous figures. These profiles are unaffected by the Coriolis force. The Coriolis force leads to a transverse tilt that is antisymmetric about the central axis. The appearance of the interface in three dimensions is illustrated in Figures 7a to 7d with views at quarter-cycle intervals. The progress of the surge as well as changes in transverse tilt can be seen. These are Kelvin waves circling the basin in an anticlockwise direction. There is a train of short-period waves following the surge. The latter are the internal expression of surface seiches that have been excited by the surface component of the internal surge.

9. Steady Upwelling

The epilimnion usually overlies the hypolimnion at all locations in Lake Champlain when it is stratified. However, when wind velocity remains high for an extended period of time, the thermocline may tilt sufficiently to intersect the surface. When that occurs, the epilimnion will be absent over the upwind end of the lake, and the hypolimnion will be exposed at the surface, promoting exchange of heat and gases between the atmosphere and the colder deep water.

A simple analytical model illustrates upwelling under steady conditions and provides an estimate for its extent in this lake. Consider the case of a constant wind blowing over a two-layered lake in a rectangular basin. Subtraction of (10) from (12) yields a relation for interface slope,

$$\frac{dh_2}{dy} = \frac{\tau_i - \tau_f}{g'\rho_2(H_2 + h_2)} - \frac{\tau_a - \tau_i}{\rho_1(H_1 - h_2)}, \tag{14}$$

where it is assumed that $h_1 \ll h_2$. Again, as in the numerical model, τ_i is considered to be negligibly small. Bottom friction is also neglected, since it is generally found in the application of other steady storm surge models of this type that $\tau_f/\tau_a \approx 0.1$ [*Bretschneider*, 1967]. The Earth's rotation has little effect in this case, since Ekman [1905] showed that for an enclosed sea or lake impelled over its whole area by the same wind, the surface slope closely follows the wind's direction under steady conditions when the vertically averaged current is nil.

For the boundary condition, $h_2 = H_1$ at $y = 0$, as shown in Figure 8, the solution is

$$h_2 = H_1 - \sqrt{\frac{2\tau_a y}{\rho_1 g'}}. \tag{15}$$

To find the length l of the shortened upper layer, we need the further constraint of volume conservation,

$$\int_0^l (H_1 - h_2)\, dy = H_1 L. \tag{16}$$

Elimination of h_2 between (15) and (16) gives a relation for the length of the shortened upper layer,

$$l^3 = \frac{9}{8}\frac{\rho g'}{\tau_a} H_1^2 L^2. \tag{17}$$

A minimum steady wind speed is required for upwelling to begin. This critical wind speed is the value at which the upper layer thickness goes to zero at the upwind end. Then the length of the upper layer just equals the basin length, that is $l = L$. It is of interest to calculate this minimum wind speed for Lake Champlain. Representative values for Lake Champlain are $\rho = 10^3$ kg/m^{-3}, $g' = 0.01$ m/s^2, $H_1 = 25$ m, and $L = 80$ km. Substitution into (17) gives a critical stress, $\tau_a = 0.088$ N/m^2, which corresponds to a critical wind speed of 5.2 m/s. Thus light winds, if they persist over sufficient time, may produce upwelling. For wind speeds only slightly greater than the critical value, a considerable expanse of lower layer may be exposed. A wind speed of 6 m/s, corresponding to a stress of $\tau_a = 0.119$ N/m^2, leads to a length of $l = 72$ km for the shortened upper layer (Figure 8). The exposed lower layer thus extends for 8 km at the upwind end. So steady winds with speeds of only 6 m/s result in exposure of the lower layer to the atmosphere over nearly 10% of the length of the lake. Steady conditions are rarely if ever reached in this lake, so this can only be considered a rough upper limit under these selected conditions.

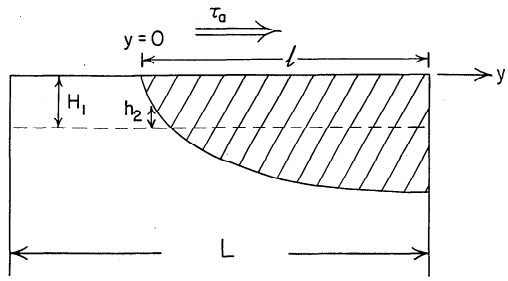

Figure 8. Longitudinal cross section of steady upwelling in a two-layered analytical lake model forced by a steady wind. At the upwind end the deep layer is exposed to the atmosphere.

The assumption of negligible bottom stress in this example is equivalent to an assumption of an infinitely deep lower layer. This assumption could be questioned in the case of Lake Champlain, where the lower layer depth is of the same order as the upper layer depth. However a more complete solution of (14), obtained numerically and not described here, that included the effects of bottom friction and finite depth for the lower layer, was found to be close to that of the simple analysis given above. For example, for a lower layer depth of 50 m and bottom stress which is 10% of wind stress, the critical stress is 0.085 N/m^2.

10. Transient Upwelling

When winds cease after producing a steady state profile like that in Figure 8, there is a transition from wind-driven to buoyancy-driven flow. Gravity currents forced by horizontal density differences will redistribute the mass in each layer, leveling the surface and interface. Some insight into the role of gravity currents in readjustment can be obtained from laboratory studies. Gravity currents under natural and laboratory conditions have been reviewed by *Simpson* [1982, 1997]. Recovery from upwelling is expected to resemble the gravity current that occurs after a light fluid is released from behind a lock gate to flow over the top of a heavier fluid.

Downwelling, the inverse of upwelling, may occur at the downwind end of a lake after a period of strong winds. In this case the thermocline intersects the bottom rather than the surface. When the upper layer is deeper than the lower layer, recovery from downwelling will take the form of a gravity current along the bottom.

When there is downwelling at one end and upwelling at the other end of a basin, recovery will resemble the lock-exchange problem in which two fluids of different densities but equal depths are initially separated by a barrier. After the barrier is removed, the two fluids flow over and under each other to seek a new equilibrium as superposed layers. Experiments and analytical theory for adjustment in a rotating system following removal of a lock gate that initially separates two fluids of different densities have been presented by *Hunkins and Whitehead* [1992].

Time-dependent upwelling and downwelling behavior may be simulated with the numerical two-layer model described earlier. In the numerical model, two layers must be present at all locations. To ensure presence of an upper layer in the model, its depth is limited to a minimum thickness, usually 1 m.

Transient upwelling can be seen in the numerical model shown in Figure 6b. Lake motion is forced by a wind burst of 10 m/s that continues for 12 hours. The surface layer at the extreme upwind end thins rapidly and effectively vanishes 12 hours after onset. The surface layer later flows back and reestablishes itself at the upwind end after 20 hours have elapsed.

11. Response to Realistic Forcing

The two-layer numerical model described here is a particularly simple one and was originally intended for studying only the effects of idealized wind forcing on long, narrow lakes. The simplifying assumptions involved were originally thought to make the model of limited use in practical interpretation of thermocline oscillations observed in Lake Champlain. Therefore it was pleasing to find that the two-layered model with a rectangular basin is capable of reproducing isotherm depths in reasonable agreement with actual measurements when it is forced with actual wind data rather than with idealized wind impulses.

Hourly wind data recorded at Burlington International Airport were used to drive the model. These are the only wind data available for this region during the period of investigation. Winds are expected to be ducted along the lake axis by the shoreline topography, and only the north-south component is used. Since the size of synoptic weather systems is generally much larger in area than the immediate lake region, it appears reasonable to assume that winds are approximately uniform over the lake, a condition that is forced by data limitations. In the future the assumption that winds from a single station are representative will be tested when additional wind recording sites become available.

Time series of interface depths for September 1993 were generated with the two-layer model for locations corresponding to the Valcour Island and Thompsons Point mooring sites. Although only the results for September are used, the model runs were all begun on August 29, 1993, to allow for initial adjustment.

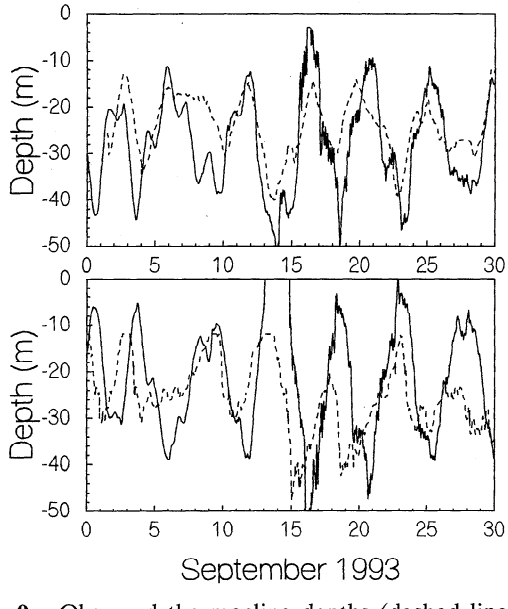

Figure 9. Observed thermocline depths (dashed line) compared with model thermocline depths (solid line) for the linear model. The free period of the model is 109 hours. The rectangular basin is 80 km long, 5 km wide, and 75 m deep; H_1 = 25 m, and H_2 = 50 m. (top) Valcour Island site. The thermocline is represented by the 16°C isotherm. (bottom) Thompsons Point site. The thermocline is represented by the 10°C isotherm.

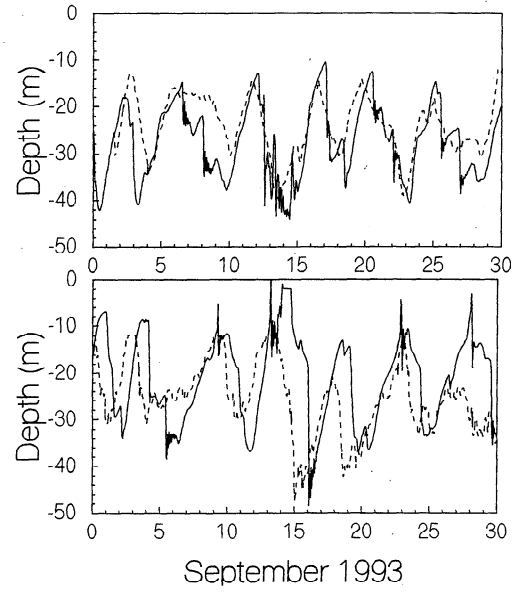

Figure 10. As in Figure 9, but for the nonlinear model.

The model was linearized for an initial comparison between computed interface depths and measured depths of isotherms in the thermocline (Figure 9). The 16°C isotherm was chosen as representative of the thermocline at Valcour Island and the 10°C isotherm was used at Thompsons Point. This choice of two different isotherms reflects the slightly different mean thermal profiles at the two locations. Nonlinear terms in the equations were dropped for this linear run. In the momentum equation the inertial nonlinear term was omitted, and depth remained constant in the stress term. Depth was also held constant in the volume transport Q of the continuity equation.

At long periods there is reasonable general agreement between the major observed isotherm oscillations and the model interface for both locations. However, for periods less than 4 days agreement is not as satisfactory. Also, amplitudes in the model exceed observed amplitudes by up to 15 m, and there is only fair agreement in phase. Nevertheless, the agreement is considered to be quite good given the simplicity of the model. This indicates that the most essential physics has been included. It should be noted that tuning of the model was kept to a minimum. Parameters were chosen to be representative of Lake Champlain. The drag coefficients for water and wind are standard values as described earlier. The higher-frequency oscillations of the model interface occurring in the second half of the month are evidently the interfacial expression of surface seiches.

When the nonlinear terms are retained, the fit is marginally improved (Figure 10). Amplitudes come into closer agreement, but phases are not altered much. Computer runs were made to test separately the effect of each nonlinear component. These runs showed that it is nonlinearity in the continuity equation which is primarily responsible for the slightly improved fit of the nonlinear model.

Limited sensitivity testing was done on some of the other

adjustable parameters. The values used in producing Figure 10 produced the best fit of any tested. Layer depths are 25 m for the epilimnion and 50 m for the hypolimnion, with a density contrast of 1 kg m^{-3}. The free period in this case is 109 hours, which is close to the period generally accepted for the first internal mode in this lake. The agreement with observations for the uniform-breadth model suggests that details of shallow coastal topography in the lake are unimportant for motions in the axial deep channel. Large oscillations are apparently guided by this channel. The selected basin depth of 75 m is intermediate between the mean depth of 29 m and the greatest depth of 122 m for the Main Lake and was chosen to represent the deep channel.

It is perhaps not surprising that a combination of length, layer thickness, and density contrast for the model that yields a free period in the vicinity of 100 hours produces reasonable agreement with observations. There will be resonance and maximum response when the period of the driving force and the natural period of the basin match each other. The fluctuating wind field has a broad spectral maximum associated with the passage of synoptic weather systems. Most of the wind energy is found between periods of 3 and 5 days. Since the 4-day period of the first internal mode of Lake Champlain lies within this band, there is abundant wind energy available to excite this mode. What is striking is the relatively good agreement in both amplitude and phase for such a simple model.

These are continuously forced motions. Since there is a close correspondence between the forcing period and the internal free period, there is no opportunity to develop free motion before another wind change occurs. Thus these are not internal seiches insofar as that term represents free oscillations. The idealized wind bursts used earlier in this paper produce results quite different from the experiments using actual winds, since there is time for free oscillations to occur after the idealized wind impulse ceases.

This simple numerical model evidently incorporates the basic physics involved in the 4-day oscillations. The important features are a two-layered fluid in a rectangular basin with an internal free period of about 100 hours which is driven by fluctuating winds. The assumption that winds based on recordings made several kilometers inland represent winds over the entire lake proves adequate for this level of modeling.

One aspect in which the nonlinear model results do not agree with observations needs comment. Internal surges with vertical fronts which appear in the numerical model results shown in Figure 10 have almost no counterpart in the recorded data. The steep fronts and spikes in the model results must be limited in the actual lake by some factor not included in the model, either dispersion or friction. The fronts in the model are followed by short-period oscillatory wave trains, which appear in Figure 10 as dark unresolved smudges. These wave trains are internal counterparts of surface seiches. Higher resolution of these results, not shown here, reveals the period of these surface seiches to be about 2 hours, in agreement with linear theory for a basin of these dimensions. However, one case of a surge with a following wave train is seen in both field data and model on September 14.

Upwelling occurred in the numerical model at Thompsons Point on September 14. Since the shallowest instrument was at a depth of 11 m, there is no information on actual isotherm behavior at depths less than 11 m. It is not certain that the hypolimnion was exposed at the surface at that time but the 10°C isotherm did rise to less than 11-m depth, and it is quite possible that it did reach the surface on that date in agreement with the model results.

12. Discussion

Numerical experiments using idealized short wind bursts for forcing show how transient winds first thicken the epilimnion at the downwind end. After the wind ceases, an internal surge develops that travels from the downwind end to the upwind end, where it is reflected. However, these results show little resemblance to behavior of the thermocline in this lake under actual wind forcing, which is continuously varying. Clear examples of reflected waves are not evident in the recordings. Forcing with continually fluctuating winds based on recorded data does produce model results closely resembling thermocline oscillations. These synoptic winds have a broad spectrum centered about the internal first-mode period of about 100 hours. The free period of the lake is seen to be a key factor in determining response in the period range from ~1 day to 1 week. In this range, lake motions are driven primarily by wind. The model has been shown to be effective over a time span of 1 month. Over longer time spans beyond the scope of this paper, seasonal changes in heat flux not included here will be important contributors to density change.

A number of assumptions made here need further examination in future modeling. Restriction to one dimension is an obvious limitation, and extension to three dimensions would be an improvement yielding current and thermocline behavior in the numerous bays and irregular deep basins of the lake. Another limitation of the model is use of vertical end walls. The actual lake bottom inclines gradually at the ends, so that the thermocline intersects the sloping bottom at a small angle rather than at a right angle as in the model. Furthermore, the ends of the Main Lake as defined here are not completely closed and have some communication with water bodies outside the Main Lake. Further improvement could also be made by incorporating better wind data. Some of the difference between model results and observation may originate in the inadequacy of a single source of wind data for the entire lake. The winds used here were recorded at a single station located several kilometers inland. A recording station recently installed at Colchester Reef will provide more representative wind data for future investigations. Finally, the role of dispersive effects in long narrow water bodies needs better understanding.

Acknowledgments. This study was supported by the Vermont Waters Resources Research Center, by the Great Lakes Environmental Research Laboratory of the National Ocean and Atmosphere Administration, by the Middlebury College, and by the funds of U. S. Geological Survey, grant 14-08-0001-G2050. The authors are indebted to two anonymous reviewers for constructive comments that resulted in improvements to the paper. Lamont-Doherty Earth Observatory contribution 5785.

References

Bretschneider, C., Storm surges, in *Advances in Hydroscience*, vol. 4, edited by V. T. Chow, pp. 341–418, Academic, San Diego, Calif., 1967.

Csanady, G., Hydrodynamics of large lakes, *Annu. Rev. Fluid Mech.*, *7*, 397–419, 1975.

Defant, A., *Physical Oceanography*, Vol. II, Pergamon, Tarrytown, N. Y., 1961.

Ekman, V. W., On the influence of the Earth's rotation on ocean currents, *Ark. Math. Astron. Fys.*, *2*(11), 1905.

Farmer, D., Observations of long nonlinear internal waves in a lake, *J. Phys. Oceanogr.*, *8*, 63–73, 1978.

Hunkins, K., and M. Fleigel, Internal undular surges in Seneca Lake: A natural occurrence of solitons, *J. Geophys. Res.*, *78*, 539–548, 1973.

Hunkins, K., and J. Whitehead, Laboratory simulation of exchange through Fram Strait, *J. Geophys. Res.*, *97*(C7), 11,299–11,321, 1992.

Hutchinson, G. E., *A Treatise on Limnology*, 336 pp., John Wiley, New York, 1957.

Imberger, J., and P. Hamblin, Dynamics of lakes, reservoirs and cooling ponds, *Annu. Rev. Fluid Mech.*, *14*, 153–187, 1982.

Kowalik, Z., and T. Murty, *Numerical Modeling of Ocean Dynamics*, 481 pp., World Sci., Singapore, 1993.

Mortimer, C., Strategies for coupling data collection and analysis with dynamic modelling of lake motions, in *Hydrodynamics of Lakes*, edited by W. Graf and C. Mortimer, 183–222, Elsevier, New York, 1979.

Myer, G. E., and G. K. Gruendling, *Limnology of Lake Champlain, Lake Champlain Basin Study*, *30*, 407 pp., New England River Basins Comm., Burlington, Vt., 1979.

Prigo, R. B., T. O. Manley, and B. S. H. Connell, Linear, one-dimensional models of the surface and internal standing waves for a long and narrow lake, *Am. J. Phys.*, *64*(3), 288–300, 1996.

Simons, T. J., Verification of numerical models of Lake Ontario, I, Circulation in spring and early summer, *J. Phys. Oceanogr.*, *4*, 507–523, 1974.

Simons, T. J., Verification of numerical models of Lake Ontario, II, Stratified calculations and temperature changes, *J. Phys. Oceanogr.*, *5*, 98–110, 1975.

Simpson, J. E., Gravity currents in the laboratory, atmosphere, and ocean, *Annu. Rev. Fluid Mech.*, *14*, 213–234, 1982.

Simpson, J. E., *Gravity Currents in the Environment and the Laboratory*, 244 pp., Cambridge Univ. Press, New York, 1997.

Thorpe, S., Near-resonant forcing in a shallow two-layer fluid: A model for the internal surge in Loch Ness?, *J. Fluid Mech.*, *63*(3), 509–527, 1974.

Turner, J., *Buoyancy Effects in Fluids*, 367 pp., Cambridge Univ. Press, New York, 1973.

Ursell, F., The long-wave paradox in the theory of gravity waves, *Proc. Cambridge Philos. Soc.*, *49*, 685–694, 1953.

Welander, P., Numerical prediction of storm surges, *Adv. Geophys.*, *8*, 315–379, 1961.

Whitham, G. B., *Linear and Nonlinear Waves*, 636 pp., John Wiley, New York, 1974.

K. Hunkins, Lamont-Doherty Earth Observatory, Columbia University, P. O. Box 1000, Palisades, NY 10964. (e-mail: hunkins@ldeo.columbia.edu)

P. Manley, Department of Geology, Middlebury College, Middlebury, VT 05753.

T. O. Manley, Marine Research Corporation, 8 Nedde Lane, Middlebury, VT 05753.

J. Saylor, NOAA Great Lakes Environmental Research Laboratory, 2205 Commonwealth Boulevard, Ann Arbor, MI 48105-1593.

(Received June 16, 1997; revised March 3, 1998;
accepted April 9, 1998.)